Frontiers in Bioscience Landmark

Front. Biosci. (Landmark Ed) **2026**; 31(7): 51619
https://doi.org/10.31083/FBL51619

Original Research

Arp2/3 Inhibition Synergizes With PARP Inhibitors by Impairing Homologous Recombination in Gastric Cancer Cells

Wenlong Li[1,2,†], Xinyue Pei[1,3,†], Yongpei Li[1,3], Yanji Lu[1,2], Xian Hong[1], Ming Sui[1], Qiang Li[1,2], Xueying Sun[4], Jingqiu Wang[4], Enming Zhang[4], Yihan Liu[4], Tao Wang[1,2], Jing Xu[4,*], Zhihui Deng[1,*]

[1]Laboratory of Protein Structure and Function, Institute of Medicine and Pharmacy, Qiqihar Medical University, 161006 Qiqihar, Heilongjiang, China
[2]School of Medical Technology, Qiqihar Medical University, 161006 Qiqihar, Heilongjiang, China
[3]School of Basic Medical Sciences, Qiqihar Medical University, 161006 Qiqihar, Heilongjiang, China
[4]Department of Gastroenterology, The First Hospital of Qiqihar, 161005 Qiqihar, Heilongjiang, China
*Correspondence: xujing19760713@163.com (Jing Xu); deng.zhihui@qmu.edu.cn (Zhihui Deng)
[†]These authors contributed equally.
Academic Editor: Sung Eun Kim
Submitted: 8 March 2026 Revised: 3 June 2026 Accepted: 10 June 2026 Published: 17 July 2026

Abstract

Background: Poly(ADP-ribose) polymerase inhibitors (PARPi) have shown limited efficacy in gastric cancer, primarily due to the rarity of inherent homologous recombination (HR) deficiency. The nuclear Arp2/3 complex was recently implicated in DNA double-strand break repair via HR. Here, we investigate whether pharmacological inhibition of Arp2/3 can induce a functional HR-deficient state to synergize with PARPi in gastric cancer cells. **Methods:** HR repair efficiency was assessed using a direct repeat green fluorescent protein (DR-GFP) reporter assay in HEK-293T cells following Arp2/3 inhibition with CK666, siRNA-mediated knockdown, or CRISPR/Cas9-mediated knockout of ACTR2/ACTR3. HGC-27 and AGS gastric cancer cells were treated with CK666 alone and in combination with olaparib or niraparib. Cell viability and synergy were evaluated by Cell Counting Kit-8 (CCK-8) and clonogenic assays (n = 3 independent experiments). DNA damage and apoptosis were assessed by immunofluorescence for gamma H2A histone family member X (γH2AX) foci (≥100 cells per condition) and Western blot analysis for cleaved PARP. **Results:** Arp2/3 inhibition with CK666 significantly impaired HR repair efficiency in the DR-GFP assay ($p < 0.01$). This effect was recapitulated by genetic knockdown or knockout of ACTR2/ACTR3. CK666 alone exerted minimal cytotoxicity, but synergized with both olaparib and niraparib to suppress proliferation (Combination Index <1), reducing the half-maximal inhibitory concentration (IC_{50}) of PARPi by approximately threefold. Combination treatment markedly enhanced γH2AX foci formation ($p < 0.0001$) and increased the level of cleaved PARP compared with either monotherapy. **Conclusions:** Inhibition of Arp2/3 compromises HR repair capacity, thereby creating a synthetic lethal interaction with PARP inhibition in gastric cancer cells. This combination strategy represents a promising therapeutic approach to broaden the clinical utility of PARPi in HR-proficient tumors and may also enable dose reduction to mitigate associated toxicities.

Keywords: stomach neoplasms; poly(ADP-ribose) polymerase inhibitors; actin-related protein 2-3 complex; homologous recombination; synthetic lethality

1. Introduction

Gastric cancer remains a critical global public health challenge. According to the most recent estimates from the World Health Organization's International Agency for Research on Cancer (IARC), it ranks as the fifth most commonly diagnosed cancer and the fifth leading cause of cancer-related death worldwide, with approximately 970,000 new cases reported in 2022 [1]. Furthermore, the epidemiology of gastric cancer is evolving, with a concerning trend toward earlier onset. An analysis of one million patient records from 1980 to 2019 published in 2023 revealed a rising incidence rate among individuals aged <40 years [2]. The dismal prognosis associated with gastric cancer stems primarily from the high rate of post-therapeutic recurrence and the limited efficacy of conventional chemotherapy [3]. While advances in radiotherapy, chemotherapy, and neoadjuvant therapies have contributed to modest improvements in survival rates, the clinical benefits are often constrained, and the frequent emergence of drug resistance poses a significant barrier to durable treatment success [4]. Consequently, there is a pressing and unmet need for the development of safer, more effective pharmacological agents and novel therapeutic strategies to expand the clinical options and improve outcomes for patients with gastric cancer.

There are at least 17 members of the conserved poly(ADP-ribose) polymerase (PARP) family. PARP1 is the most studied and functionally predominant isoform, responsible for approximately 90% of total cellular PARP activity [5]. It acts as a critical DNA damage sensor and repair enzyme, rapidly binding to single-strand breaks (SSBs) and catalyzing poly(ADP-ribose)ation (PARylation) using

NAD+ as a substrate [6]. The resulting poly(ADP-ribose) (PAR) chains promote chromatin decompaction through electrostatic repulsion and serve as a molecular scaffold for the recruitment of downstream repair factors [7]. PARP1 is integral to SSB repair, participating in nearly every step of the process [8]. Its rapid recruitment and activation facilitate the assembly of repair complexes: XRCC1 recognizes PAR chains and acts as a scaffold to recruit key enzymes (e.g., PNKP, Aprataxin, POLB, and LIG3) and complete the repair process [9]. Efficient repair of the numerous SSBs that occur daily is crucial to prevent collapse of the replication fork and transcription arrest, thereby maintaining genomic stability and averting associated pathologies [10].

The therapeutic application of Poly(ADP-ribose) polymerase inhibitors (PARPi) is founded on the concept of synthetic lethality in tumors that are deficient for homologous recombination (HR). These inhibitors competitively bind the PARP1 catalytic site and block its activity [11]. Inhibition leads to the persistence of SSBs, which are converted into cytotoxic double-strand breaks (DSBs) during DNA replication [12]. While HR-proficient cells can repair these DSBs, tumors with HR defects, such as those harboring mutations in BRCA1/2, cannot. This failure leads to genomic instability and ultimately cell death [13]. Clinically, this strategy has proven successful in treating advanced ovarian, breast, pancreatic, and prostate cancers with BRCA mutations or other HR deficiencies [14]. However, dose-limiting toxicities and the frequent development of resistance remain significant challenges to the broader utility of PARPi [15].

In recent years, the nuclear localization of the Arp2/3 complex and its upstream activators, and their regulatory functions in DNA damage repair, have gradually been elucidated and have attracted significant attention [16]. Specifically, the nuclear Arp2/3 complex is recruited to DSB sites. Upon activation by upstream signals, it catalyzes the formation of actin filaments, which in turn drive the movement of DSBs from heterochromatin regions toward the nuclear periphery to facilitate repair [17]. Concurrently, studies have demonstrated that this complex localizes to DNA ends during HR repair, promoting DNA end resection and subsequent HR repair by mediating the bundling of damaged DNA molecules [18]. These findings have established the crucial role of the nuclear Arp2/3 complex in the DSB response. However, several critical scientific questions remain: can the Arp2/3 complex itself be a viable target for anticancer therapeutics? Furthermore, given its function within the HR repair pathway, could inhibitors targeting Arp2/3 synergize with PARP1 inhibitors to induce synthetic lethality, thereby offering a novel combinatorial therapeutic strategy for cancers, including gastric cancer? This constitutes a hitherto unaddressed, yet highly promising area of research.

To address this gap, we sought to elucidate whether pharmacological inhibition of the Arp2/3 complex could be leveraged to induce a state of functional HR deficiency, thereby sensitizing gastric cancer cells to PARPi. In this study, we explored the therapeutic potential of combining the specific Arp2/3 complex inhibitor CK666 with two clinically relevant PARPi, olaparib and niraparib. We demonstrate that CK666 effectively compromises the cellular HR repair capacity. This induced repair defect creates a robust synthetic lethal interaction with PARP inhibition, leading to exacerbated accumulation of DNA damage and synergistic suppression of gastric cancer cell proliferation. Our findings establish Arp2/3 as a viable therapeutic target and delineate a novel combinatorial strategy to expand the efficacy of PARPi. This approach offers a promising avenue for treating gastric cancers that are otherwise resistant to PARP monotherapy. Moreover, it may also allow the use of reduced doses of PARPi in clinical settings, potentially mitigating their dose-limiting toxicities and overcoming mechanisms of resistance.

2. Materials and Methods

2.1 Cells, Reagents, and Plasmids

The human gastric carcinoma cell lines HGC-27 and AGS, along with the HEK-293T cell line, were purchased from the National Infrastructure of Cell Line Resource. HGC-27 cells (SCSP-5263, Cell Bank of Chinese Academy of Sciences) and AGS cells (TCHu232, Cell Bank of Chinese Academy of Sciences) were used within 10 passages; HEK-293T cells (1101HUM-PUMC000091, Cell Resource Center, Peking Union Medical College) were used within 20 passages. All cell lines (HEK-293T, HGC-27 and AGS) were validated by STR profiling and tested negative for mycoplasma contamination. Isogenic ACTR2 (Arp2) and ACTR3 (Arp3) knockout (KO) cell lines were generated in this study. All cells were maintained at 37 °C in a humidified atmosphere of 5% CO_2. HGC-27, AGS, and their derived knockout cells were cultured in RPMI-1640 medium, while HEK-293T and its derived knockout cells were cultured in DMEM; each medium was supplemented with 10% fetal bovine serum (FBS). The PARPi olaparib (HY-10162) and the Arp2/3 complex inhibitor CK666 (HY-16926) were obtained from MedChemExpress (Monmouth Junction, NJ, USA), while the PARPi niraparib (1038915-60-4) was obtained from Aladdin (Shanghai Aladdin Biochemical Technology, Pudong New Area, Shanghai 201206, China). Antibody against gamma H2A histone family member X (γH2AX) (05-636) was purchased from Merck (Merck KGaA, Darmstadt, Germany), antibodies against Arp2 (10922-1-AP), Arp3 (13822-1-AP), and GAPDH (60004-1-Ig) from Proteintech Group (Rosemont, IL, USA), antibodies against cleaved PARP (#5625) and Histone H2AX (#7631) from Cell Signaling Technology (Danvers, MA, USA), and Alexa Fluor 488-conjugated goat anti-mouse IgG (A-11001) from Thermo Fisher Scientific (Waltham,

MA, USA) and Goat Anti-Rabbit IgG H&L (511203) and Rabbit Anti-Mouse IgG H&L (HRP) (701051) from Chengdu Zen Bioscience (Chengdu, Sichuan, China). The reporter plasmids DR-GFP (26475) and pCBASceI (26477) were obtained from Addgene (Watertown, MA, USA). Plasmids pCI2-HA-mCherry and pSpCas9(BB)-2A-Puro (PX459) V2.0 were generously provided by Professor Daniel D. Billadeau (Mayo Clinic College of Medicine, MN, USA). Puromycin (HY-B1743) and Cell Counting Kit-8 (CCK-8; HY-K0301) were purchased from MedChemExpress (Monmouth Junction, NJ, USA), Lipofectamine 3000 (L3000015) and Hoechst 33342 (H3570) from Thermo Fisher Scientific (Waltham, MA, USA), and siRNA-mate (G04002) from GenePharma (Shanghai, China). Linear polyethylenimine (PEI; 23966) was purchased from Polysciences (Warrington, PA, USA) and was prepared as a 2 mg/mL stock solution in sterile water.

2.2 Cell Viability Assay

Cell viability was assessed using the CCK-8 assay. Cells were seeded in 96-well plates (3000 cells/well) and allowed to adhere overnight. They were then treated with the indicated concentrations of olaparib, niraparib, or CK666 for 72 h. Subsequently, CCK-8 reagent was added to each well to a final concentration of 10% (v/v), followed by incubation for 1 h (AGS cells) or 3 h (HGC-27 cells). Absorbance at 450 nm was measured using a Tecan Spark microplate reader (Tecan Spark 10M, Grödig, Salzburg, Austria). Relative viability was normalized to untreated control wells.

2.3 Colony Formation Assay

Cells were plated in 6-well plates at a density of 500 cells per well and treated as specified. After 7 days of culture, colonies were fixed with 4% paraformaldehyde and stained with 0.1% (w/v) crystal violet.

2.4 siRNA Transfection

siRNAs targeting ACTR2 or ACTR3 (**Supplementary Table 1**) were transfected using siRNA-mate according to the manufacturer's protocol. Briefly, siRNA and transfection reagent were separately diluted in Opti-MEM, combined, and then incubated for 15 minutes at room temperature. Complexes were added to cells and subsequently incubated for 48 h before harvesting for analysis by Western blot to assess knockdown efficiency.

2.5 CRISPR/Cas9-Mediated Gene Knockout

sgRNAs targeting exon regions of ACTR2 or ACTR3 (**Supplementary Table 2**) were cloned into the pSpCas9(BB)-2A-Puro (PX459) V2.0 vector. Plasmids were transfected into target cells using Lipofectamine 3000 reagent (Invitrogen) according to the manufacturer's protocol. At 48 h post-transfection, positive clones were selected with puromycin for 48 h using the following cell line-specific concentrations: 2 μg/mL for HEK-293T, 1 μg/mL for AGS, and 0.66 μg/mL for HGC-27. Cells were then single-cell cloned by limiting dilution in 96-well plates. Knockout efficiency was confirmed by Western blot analysis for Arp2 and Arp3 protein loss.

2.6 Homologous Recombination Repair Assay

HR repair efficiency was assessed using the DR-GFP reporter assay in various genetic and pharmacological contexts. HEK-293T wild-type (WT) or isogenic ACTR2- or ACTR3-KO cells were seeded in 6-well plates and cultured until ~50% confluency. For siRNA-mediated knockdown, WT cells were first transfected with 45 nM ACTR2- or ACTR3-specific siRNA using the siRNA-mate transfection reagent. For pharmacological inhibition, WT cells were pretreated with 100 μM CK666 (an Arp2/3 complex inhibitor). Both siRNA transfection and drug treatment were performed 24 h prior to subsequent plasmid transfection. Following these pretreatments (or directly for KO cells and untreated controls), all cells were co-transfected with 1 μg each of the DR-GFP reporter, pCBASceI (I-SceI expression vector), and pCI2-HA-mCherry (transfection control) plasmids, using linear PEI at a DNA-to-PEI mass ratio of 1:10. Cells were harvested and analyzed by flow cytometry 48 h after plasmid transfection. HR efficiency was quantified as the percentage of GFP-positive cells within the mCherry-positive cell population. Flow cytometric gating was performed as previously described: intact cells were first gated on the FSC-A/SSC-A plot to exclude debris and doublets. From the intact cell population, a new plot was generated with FL1-H (x-axis, GFP) and FL2-H (y-axis, mCherry). Quadrant gates were positioned using the negative control (untransfected cells), with GFP single-color and mCherry single-color controls used to fine-tune discrimination.

2.7 Western Blotting

Cells were lysed in RIPA buffer supplemented with protease inhibitors. Lysates were sonicated briefly and centrifuged. Equal amounts of protein were separated by SDS-PAGE (10% or 12% gels) and transferred to PVDF membranes. Membranes were blocked with 5% BSA in TBS for 1 h and incubated overnight at 4 °C with primary antibodies, antibodies against Arp2 (10922-1-AP, 1:2000), Arp3 (13822-1-AP, 1:4000), GAPDH (60004-1-Ig, 1:2000), PARP (#5625, 1:1000), and H2AX (#7631, 1:1000), followed by incubation with appropriate HRP-conjugated secondary antibodies Goat Anti-Rabbit IgG H&L (511203, 1:10,000) and Rabbit Anti-Mouse IgG H&L (HRP) (701051, 1:10,000). Signals were detected using enhanced chemiluminescence.

2.8 Immunofluorescence

Cells grown in 24-well black-walled glass-bottom plates (Cellvis, #P24-1.5H-N) were fixed with 4% paraformaldehyde, permeabilized with 0.15% Triton

X-100, and blocked with immunofluorescence blocking buffer (PBS containing 5% goat serum, 1% glycerol, 0.1% BSA, and 0.1% fish skin gelatin). Cells were incubated overnight at 4 °C with anti-γH2AX antibody (05-636, 1:200), followed by Alexa Fluor 488-conjugated secondary antibody (A-11001, 1:200) for 1 h at room temperature in the dark. Nuclei were counterstained with Hoechst 33342. Images were acquired using a Zeiss LSM 710 confocal microscope and analyzed with ImageJ software (1.54g, National Institutes of Health, Bethesda, MD, USA). γH2AX foci were counted in at least 100 cells per condition.

2.9 Statistical Analysis

Statistical analyses were performed using GraphPad Prism software (GraphPad Prism version 10.5.0, LLC, San Diego, CA, USA). Data are presented as the mean ± SD (or SEM, as specified in figure legends). A two-tailed unpaired Student's *t*-test was used for comparisons between two groups. One-way analysis of variance (ANOVA) was performed for comparisons among more than two groups, followed by Dunnett's post hoc test for comparisons against a specified control group. A p-value of <0.05 was considered statistically significant. In the Figure legends, statistical significance is denoted as follows: ns, not significant; *$p < 0.05$; **$p < 0.01$; ***$p < 0.001$; ****$p < 0.0001$.

3. Results

3.1 Arp2/3 Deficiency Confers Gastric Cancer Cells With Sensitivity to PARP Inhibitors

Analysis of TCGA and GTEx data using GEPIA2 revealed that transcript levels of ACTR2 and ACTR3, which encode the core catalytic subunits Arp2 and Arp3 of the Arp2/3 complex, as well as the DNA repair gene PARP1, were significantly upregulated in gastric tumor tissues relative to matched normal controls (**Supplementary Fig. 1**) [19]. Integrated transcriptomic and proteomic profiles from the Human Protein Atlas (HPA) further confirmed elevated expression of Arp2, Arp3, and PARP1 proteins in the commonly used gastric cancer cell lines HGC-27 and AGS (**Supplementary Fig. 2**) [20]. Based on their high expression of these targets, HGC-27 (undifferentiated adenocarcinoma) and AGS (moderately differentiated adenocarcinoma) were selected as representative models for subsequent experiments. To determine whether the Arp2/3 complex represents a druggable vulnerability that can enhance the efficacy of PARPi, CRISPR/Cas9 was used to generate isogenic knockout models of its core catalytic subunits, Arp2 and Arp3 (encoded by ACTR2 and ACTR3, respectively), in both cell lines. Genetic ablation of either subunit resulted in concomitant loss of the other at the protein level (Fig. 1A–D), confirming effective disruption of complex integrity. This mutual reduction in Arp2 and Arp3 protein levels likely reflects the structural interdependence within the Arp2/3 complex, where unassembled subunits may be targeted for proteasomal degradation, consistent with previous reports [21]. We then tested whether Arp2/3 deficiency could hypersensitize cells to PARP inhibition. CCK-8 viability assays demonstrated that Arp2 or Arp3 KO cells exhibited significantly greater suppression of proliferation following treatment with the PARPi olaparib or niraparib compared with wild-type controls (Fig. 1E–L). To further characterize this sensitivity over time, we performed time-course CCK-8 assays (0–72 h) using the same PARPi concentrations as in Fig. 1. The results showed that Arp3 KO cells displayed a progressive and time-dependent decrease in viability compared to WT cells, with the most pronounced differences observed at 48 and 72 h (**Supplementary Fig. 3**). Given the established role of the Arp2/3 complex in promoting HR-mediated repair of DSBs [18], these findings suggest that loss of Arp2/3 function compromises HR proficiency, thereby establishing a synthetic lethal interaction with PARP inhibition in gastric cancer cells.

3.2 Arp2/3 Inhibitor Synergizes With Olaparib to Inhibit Gastric Cancer Cell Proliferation and Induce Apoptosis

Building on our findings that genetic deficiency of the Arp2/3 complex sensitizes gastric cancer cells to PARP inhibition (Fig. 1), we hypothesized that pharmacological inhibition of Arp2/3 would similarly synergize with PARP blockade. To test this, HGC-27 and AGS cells were treated with the Arp2/3 inhibitor CK666 in combination with the PARPi olaparib. Cell viability after 72 h of co-treatment was assessed by CCK-8 assay. Analysis revealed strong synergistic growth inhibition in both cell lines (Fig. 2A–D). This synergy was not attributable to additive cytotoxicity, as the concentration of CK666 used alone exhibited minimal effect on clonogenic survival (Fig. 2E–H). Dose-response analysis further demonstrated that CK666 reduced the half-maximal inhibitory concentration (IC_{50}) of olaparib by approximately threefold in both gastric cancer models (Fig. 2I,J). To determine whether the synergistic interaction induced apoptotic cell death, we examined the cleavage of PARP, a hallmark of apoptosis. Western blot analysis showed that combination treatment markedly increased the level of cleaved PARP compared to either agent alone (Fig. 2K,L), suggesting that enhanced apoptosis contributes to the observed synergistic lethality.

3.3 Arp2/3 Inhibitor Synergizes With Niraparib to Inhibit Gastric Cancer Cell Proliferation and Induce Apoptosis

To determine whether the synergistic lethality observed between CK666 and olaparib extends to other PARPi, we next evaluated the combination of CK666 with niraparib. In HGC-27 and AGS wild-type cells, a 72-h co-treatment assessed by CCK-8 assay revealed significant synergistic growth inhibition (Fig. 3A–D). This synergy was corroborated by clonogenic assays, where the combination profoundly suppressed colony formation compared to

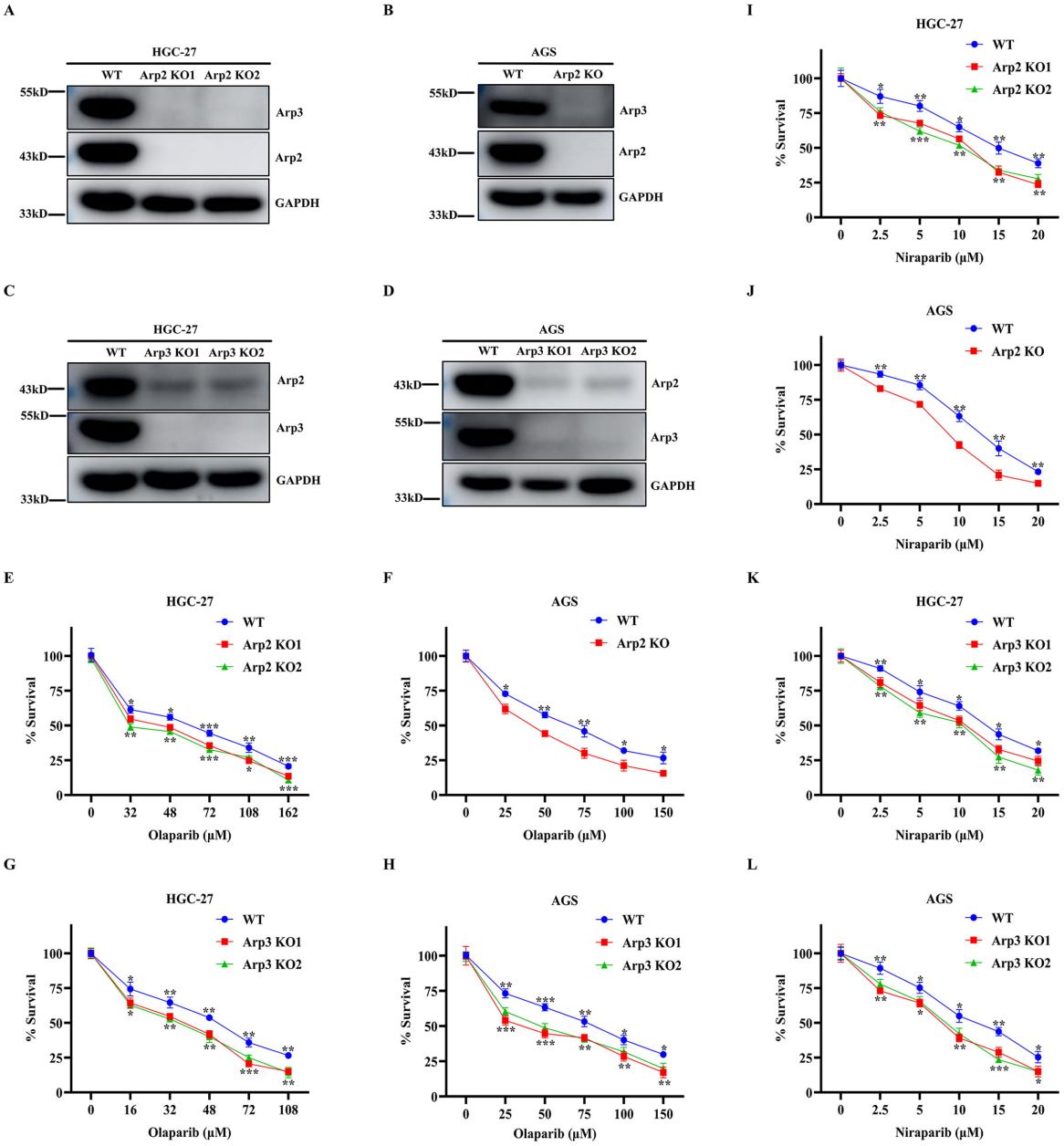

Fig. 1. Arp2/3 deficiency confers gastric cancer cells with sensitivity to PARP inhibitors. (A–D) Western blot confirmation of Arp2 or Arp3 KO in HGC-27 and AGS cells generated by CRISPR/Cas9. Blots are representative of three independent experiments. (E–L) Dose-response curves from a representative experiment showing the viability of HGC-27 and AGS cells with Arp2 or Arp3 KO treated with gradient concentrations of olaparib or niraparib for 72 h (CCK-8 assay). Similar results were obtained in three independent experiments. Data are presented as the mean ± SD. *$p < 0.05$; **$p < 0.01$; ***$p < 0.001$. PARP, Poly(ADP-ribose) polymerase; KO, knockout; HGC-27, human gastric cancer cell line 27; AGS, adenocarcinoma of the gastric stomach; CRISPR/Cas9, Clustered Regularly Interspaced Short Palindromic Repeats/CRISPR-associated protein 9; Arp2, Actin-related protein 2; CCK-8, Cell Counting Kit-8; SD, standard deviation.

either agent alone (Fig. 3E–H). Dose-response analysis further demonstrated that CK666 reduced the IC_{50} of niraparib to an extent similar to that observed with olaparib (approximately a threefold decrease) in both cell lines (Fig. 3I,J). Western blot analysis for cleaved PARP confirmed that the combinatorial treatment markedly increased apoptotic signaling compared to monotherapies (Fig. 3K,L). Collectively, these data indicate the synergy between Arp2/3 inhibition and PARP blockade is generalizable across different PARPi, with the potentiation of apoptosis being a consistent underlying mechanism.

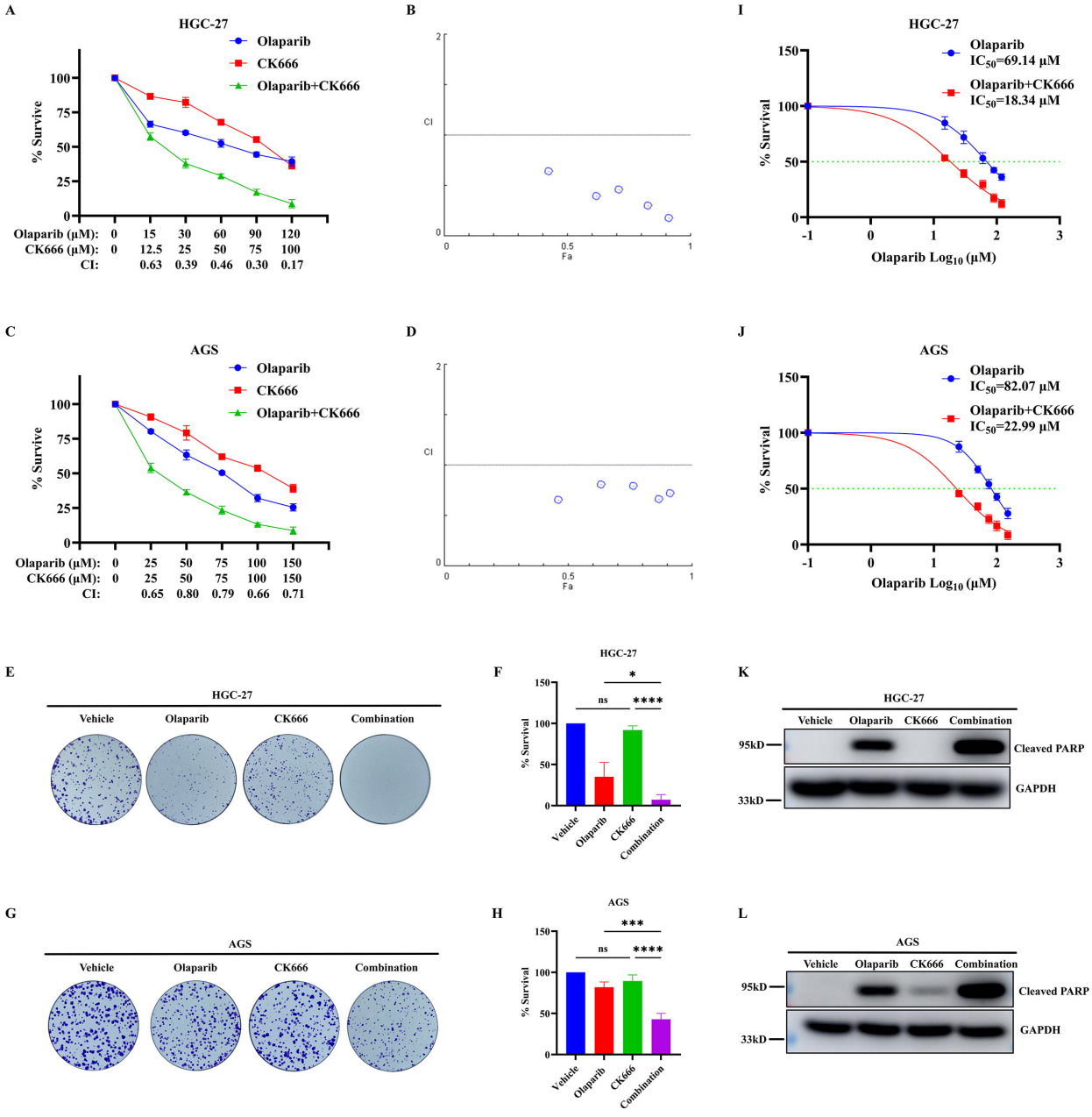

Fig. 2. Arp2/3 inhibitor synergizes with olaparib to inhibit gastric cancer cell proliferation and induce apoptosis. (A–D) Synergy analysis of CK666 and olaparib in HGC-27 and AGS cells. Cells were treated with the indicated drug combinations for 72 h, and viability was then measured by CCK-8 assay. The Combination Index (CI), where a value <1 indicates synergy, was calculated using CompuSyn software. Data are presented as the mean ± SEM of three independent experiments. (E–H) Clonogenic survival assays of cells treated for 7 days with CK666, olaparib, or the combination. HGC-27 cells were treated with 0.08 μM olaparib and/or 1.5 μM CK666. AGS cells were treated with 0.03 μM olaparib and/or 0.75 μM CK666. Representative images (E,G) and quantification (F,H) of colonies are shown. Quantification data are presented as the mean ± SD of three independent experiments. Statistical significance was determined by one-way ANOVA with Dunnett's post hoc test against the vehicle control. (ns, not significant; *$p < 0.05$; ***$p < 0.001$; ****$p < 0.0001$). (I,J) Dose-response curves of olaparib alone or in combination with a fixed concentration of CK666 (50 μM for HGC-27; 75 μM for AGS) for 72 h. Curves were fitted, and the half-maximal inhibitory concentration (IC_{50}) was derived. Data are presented as the mean ± SEM of three independent experiments. (K,L) Western blot analysis of cleaved PARP in cells treated for 24 h with CK666, olaparib, or the combination (HGC-27: 120 μM olaparib alone, or combined with 100 μM CK666; AGS: 150 μM olaparib alone, or combined with 150 μM CK666). Blots are representative of three independent experiments. SEM, standard error of the mean; ANOVA, analysis of variance.

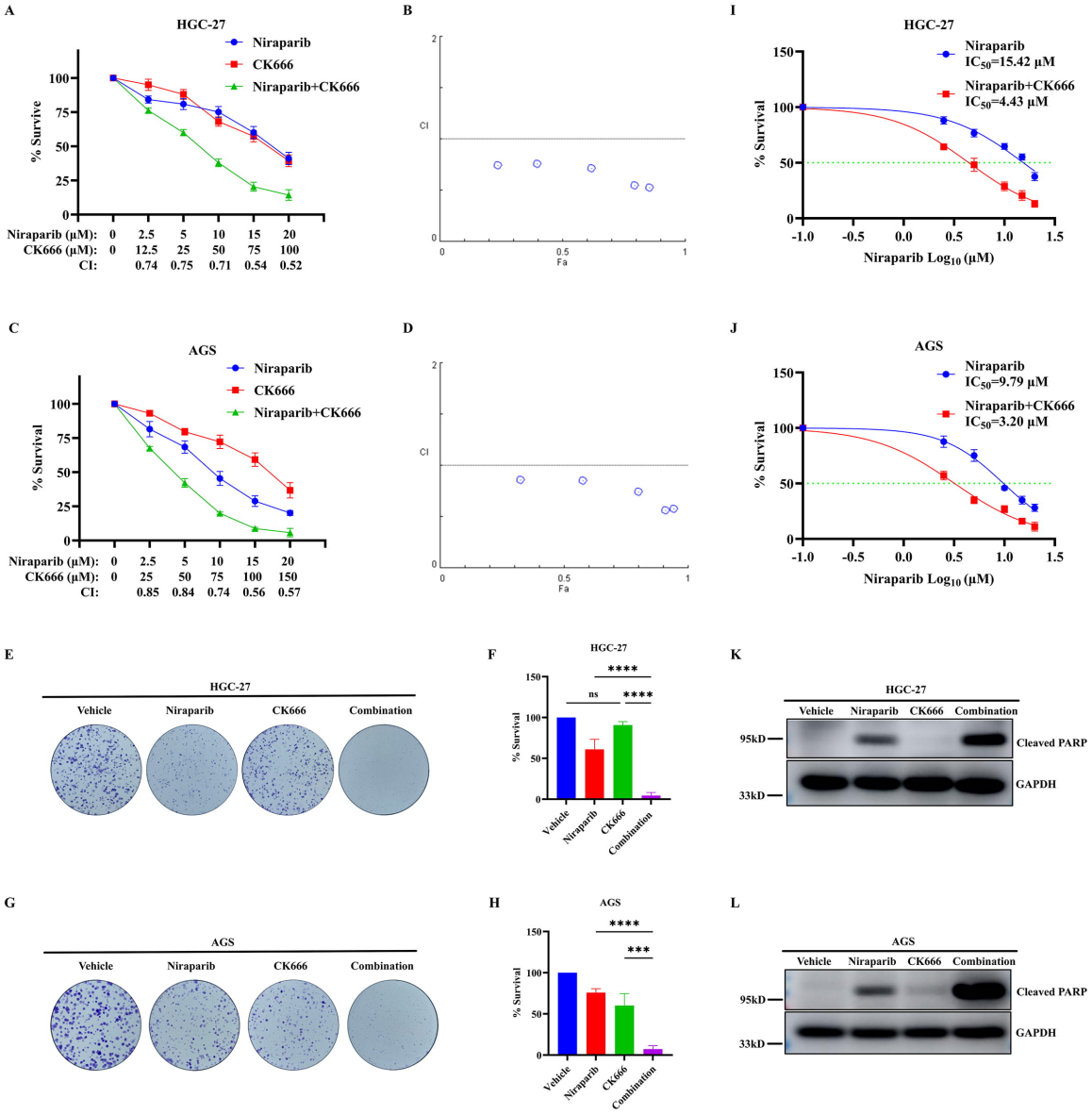

Fig. 3. Arp2/3 inhibitor synergizes with niraparib to inhibit gastric cancer cell proliferation and induce apoptosis. (A–D) Synergy analysis of CK666 and niraparib. Cells were treated and analyzed as in Fig. 2A–D. Data are presented as the mean ± SEM of three independent experiments. (E–H) Clonogenic survival assays of cells treated for 7 days with CK666, niraparib, or the combination. HGC-27 cells were treated with 0.25 μM niraparib and/or 1.5 μM CK666. AGS cells were treated with 0.125 μM niraparib and/or 1.5 μM CK666. Data are presented as the mean ± SD of three independent experiments. Statistical significance was determined by one-way ANOVA with Dunnett's test against the vehicle control (ns, not significant; ***$p < 0.001$; ****$p < 0.0001$). (I,J) Dose-response curves of niraparib alone or in combination with a fixed concentration of CK666 (50 μM for HGC-27; 75 μM for AGS) for 72 h. Data fitting and presentation are as in Fig. 2I,J. Data are presented as the mean ± SEM of three independent experiments. (K,L) Western blot analysis of cleaved PARP in cells treated for 24 h with CK666, niraparib, or the combination (HGC-27: 20 μM niraparib alone or combined with 100 μM CK666; AGS: 20 μM niraparib alone or combined with 150 μM CK666). Blots are representative of three independent experiments.

3.4 Arp2/3 Inhibition Sensitizes Gastric Cancer Cells to PARP Inhibitors by Amplifying DNA Damage Accumulation

To elucidate the molecular mechanism of synergy between Arp2/3 complex inhibitors and PARPi, we assessed drug-induced DNA damage in gastric cancer cells by monitoring the DNA DSB marker γH2AX [22]. Immunofluorescence analysis revealed that treatment with the Arp2/3 inhibitor CK666 alone did not elicit a substantial increase in γH2AX foci. However, co-treatment with CK666 and either olaparib or niraparib potently amplified γH2AX foci formation in both HGC-27 and AGS cell lines compared

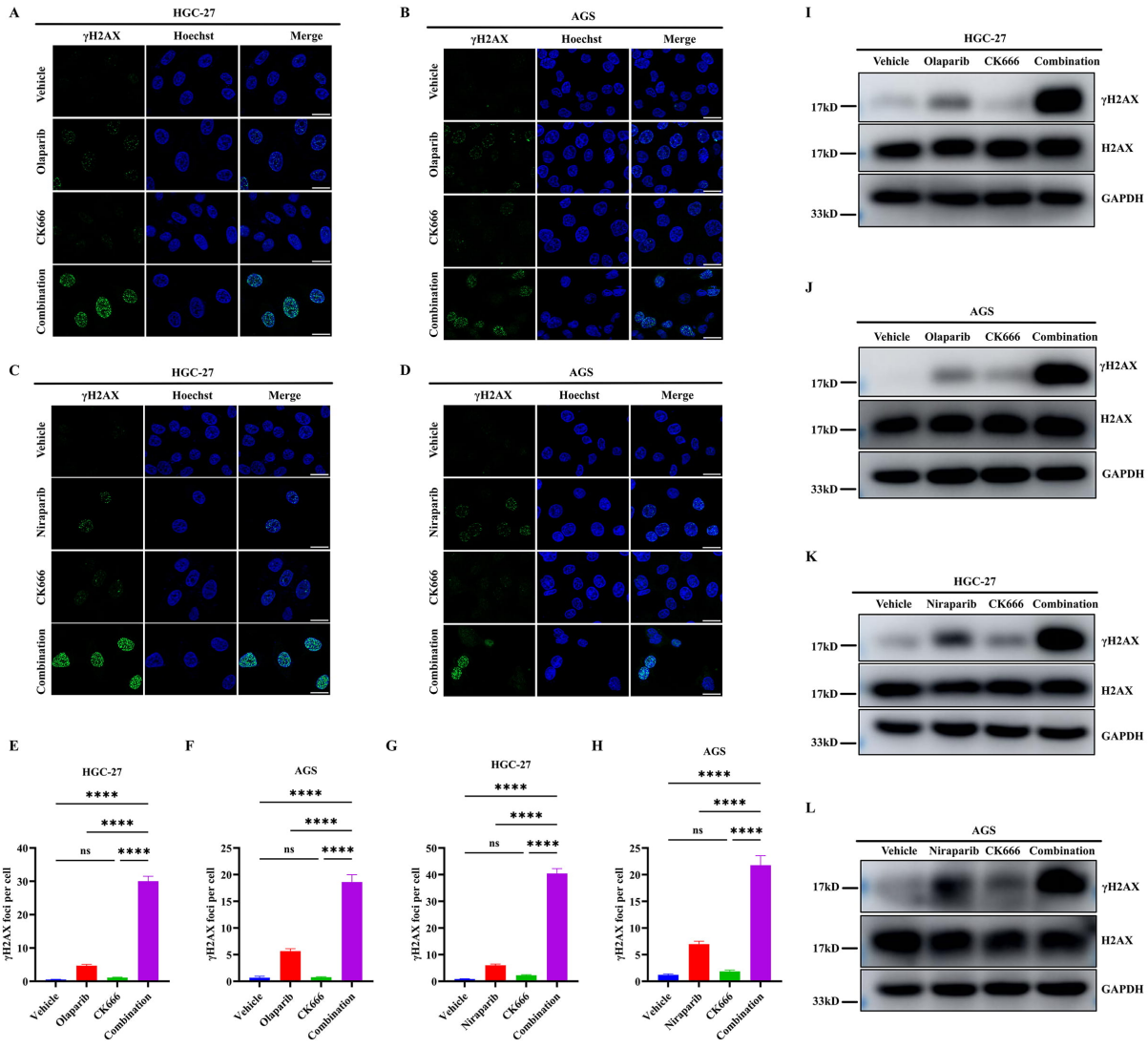

Fig. 4. Arp2/3 inhibition sensitizes gastric cancer cells to PARP inhibitors by amplifying DNA damage accumulation. (A–H) DNA damage was assessed by immunofluorescence staining for γH2AX foci in cells. HGC-27 cells were treated for 24 h with olaparib (120 μM) with or without CK666 (100 μM), or niraparib (20 μM) with or without CK666 (100 μM). AGS cells were treated for 24 h with olaparib (150 μM) with or without CK666 (150 μM), or niraparib (20 μM) with or without CK666 (150 μM). Representative images and quantification of foci per nucleus (at least 100 cells scored per condition) are shown (scale bar = 20 μm). Data are presented as the mean ± SEM of three independent experiments. Statistical significance was determined by one-way ANOVA with Dunnett's test, comparing each combination treatment to its corresponding PARPi monotherapy (ns, not significant; ****$p < 0.0001$). (I–L) Western blot analysis of γH2AX protein levels in cells treated as described in (A–H). Blots are representative of three independent experiments. γH2AX, gamma H2A histone family member X.

to PARPi monotherapy (Fig. 4A–H). This marked increase in the DNA damage response was confirmed at the protein level by Western blot analysis, which showed significantly intensified γH2AX signaling specifically in the combination treatment groups (Fig. 4I–L). Together, these data indicate that pharmacological inhibition of the Arp2/3 complex does not directly inflict severe DNA damage, but instead markedly potentiates the DNA-damaging effects of PARPi, thus providing a mechanistic basis for their synergistic interaction.

3.5 Arp2/3 Inhibition Impairs Homologous Recombination

The findings described above demonstrate that combining CK666 with PARPi results in substantial DNA damage accumulation. Given that Arp2/3-driven movement of broken chromatin ends has been implicated in HR repair [18], we employed a DR-GFP reporter system to investigate whether Arp2/3 inhibition affects HR efficiency [23]. To assess whether PARPi directly affects HR repair or modulates the effect of Arp2/3 inhibition, we performed DR-GFP

reporter assays with olaparib and niraparib. As shown in Fig. 5A–D, neither olaparib nor niraparib alone altered HR efficiency relative to the DMSO control. However, CK666 alone significantly reduced HR efficiency. Notably, compared with CK666 alone, combined treatment of CK666 and PARP inhibitors does not markedly affect HR efficiency. These data indicate that CK666 is the major driver of HR impairment, and that PARPi does not intrinsically interfere with HR, nor do they significantly exacerbate or rescue the HR defect caused by Arp2/3 inhibition. Consistent with this, siRNA-mediated transient knockdown of Arp2 or Arp3 resulted in a marked reduction in HR efficiency (Fig. 5E–J). Finally, genetic KO of Arp2 or Arp3 led to a consistent decline in HR function (Fig. 5K–P), reinforcing that the Arp2/3 complex is indispensable for maintaining robust HR function. Collectively, these results indicate that Arp2/3 inhibition disrupts HR repair. Based on the well-established synthetic lethality paradigm between PARP inhibition and HR deficiency, our data provide a mechanistic explanation for the synergy observed in gastric cancer cells, i.e., Arp2/3 inhibitors pharmacologically induce an "HR-deficient" state, thereby creating a conditional vulnerability that can be exploited by PARPi.

4. Discussion

The clinical success of PARP inhibition is firmly rooted in the synthetic lethality paradigm for tumors with inherent HR deficiency [24]. This therapeutic strategy has limited benefit for the majority of cancers that are HR proficient, including most gastric cancers [25]. Our study addresses this fundamental limitation by identifying the actin-nucleating Arp2/3 complex as a druggable vulnerability whose inhibition induces a functional HR-deficient state. We demonstrate that genetic ablation or pharmacological inhibition of Arp2/3 strongly sensitizes gastric cancer cells to PARPi like olaparib and niraparib. This synergy is mechanistically driven by the impairment of HR-mediated DNA repair, leading to exacerbated DNA damage and apoptotic cell death. By establishing Arp2/3 as a key regulator of HR proficiency, our work reveals a novel combinatorial strategy to expand the therapeutic reach of PARPi through pharmacologically-induced HR deficiency.

The observed synthetic lethal interaction is firmly grounded in the established nuclear functions of the Arp2/3 complex. Prior work has shown that Arp2/3-mediated actin polymerization facilitates the mobilization of DSBs from repressive chromatin environments and promotes DNA end resection, both of which are critical steps for efficient HR [17,18,26]. Our data directly link this molecular function to therapeutic outcome. Using a DR-GFP reporter assay, we provide direct evidence that CK666-mediated Arp2/3 inhibition, as well as genetic knockdown or KO of its core subunits, significantly compromises HR efficiency. This creates a conditional genomic instability that is selectively lethal upon PARP trapping and subsequent collapse of the replication fork. The consistency of synergy across two structurally distinct PARPi underscores the generality of this mechanism, positioning Arp2/3 inhibition as a broad strategy for PARPi potentiation.

Beyond elucidating a new mechanistic vulnerability, our findings carry significant translational implications. First, the robust *in vitro* synergy suggests that combining an Arp2/3 inhibitor with a PARPi could significantly lower the clinically effective dose of the latter. Given that hematological toxicities and fatigue associated with PARPi are often dose-limiting, such a dose-reduction strategy could markedly improve the therapeutic index and patient tolerability [27]. Second, by targeting a proximal component of the HR machinery, Arp2/3 inhibition presents a promising avenue to counteract or delay the emergence of PARPi resistance, which is frequently driven by mechanisms that restore HR function [28]. This combination strategy could therefore benefit a broader patient population, including those with initially HR-proficient tumors, or those who have developed acquired resistance.

Interestingly, in our study, pharmacological inhibition of Arp2/3 with CK666 produced a more pronounced synergistic effect with PARP inhibitors than genetic knockout of Arp2 or Arp3. Several factors may explain this discrepancy. First, residual expression of Arp2/3 in knockout cells, possibly below the detection limit of Western blotting, may still support some level of homologous recombination repair. Second, long-term culture of knockout cells may allow compensatory mechanisms to partially restore HR capacity, whereas CK666 provides rapid and complete inhibition. Third, although CK666 is widely used as a specific Arp2/3 inhibitor, potential off-target effects cannot be completely excluded and may contribute to the enhanced synergy.

While our study highlights the nuclear role of Arp2/3 in HR repair, the complex also regulates cytoplasmic processes such as cell migration, adhesion, endocytosis, and cytokinesis. Consistent with prior reports, we observed morphological changes in Arp2/3 KO cells, suggesting that cytoplasmic functions may also contribute to the phenotypes seen with CK666 treatment. Moreover, although CK666 is widely used as a specific Arp2/3 inhibitor, potential off-target effects cannot be fully excluded. Future studies using structurally distinct Arp2/3 inhibitors (e.g., CK548 or CMD-39) and additional genetic validation will be essential to confirm the specificity of the observed synergy. This observation highlights the potential translational challenge of achieving a therapeutic window in which nuclear DNA repair functions are selectively impaired without incurring toxicity from cytoplasmic inhibition. The development of next-generation, context-specific inhibitors or targeted delivery systems may therefore be essential to overcome this hurdle.

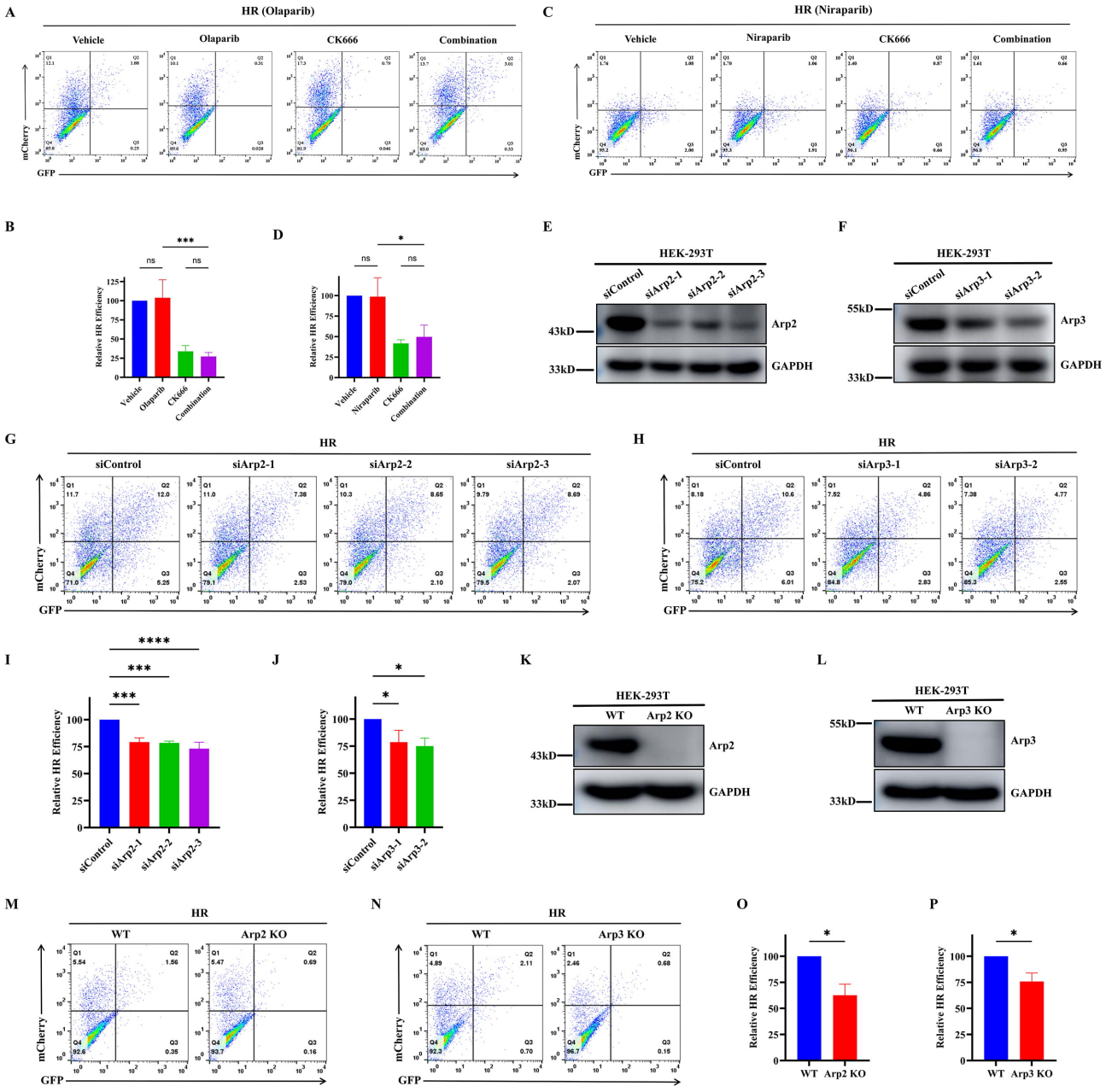

Fig. 5. Arp2/3 inhibition impairs homologous recombination. (A,C) Representative flow cytometry plots (gated on mCherry$^+$ cells) of HEK-293T cells treated for 48 h with the indicated agents (DMSO, olaparib, niraparib, CK666, or their combinations). (B,D) Quantification of homologous recombination efficiency, expressed as the percentage of GFP$^+$ cells among mCherry$^+$ cells, from three independent experiments. Data represent the mean ± SD of three independent experiments. Statistical significance was determined by one-way ANOVA with Dunnett's test. (E–J) HR efficiency following siRNA-mediated knockdown of Arp2 or Arp3. (E,F) Western blot analysis confirms depletion of Arp2 (E) or Arp3 (F), with GAPDH serving as the loading control. (G,H) Representative flow cytometry plots gated on mCherry$^+$ cells (to exclude non-transfected cells). (I,J) Quantification of HR efficiency (expressed as the percentage of GFP$^+$ cells among mCherry$^+$ cells); data represent the mean ± SD of three independent experiments. For (I,J), statistical significance relative to the siControl group was determined by one-way ANOVA with Dunnett's test. (I–N) HR efficiency in HEK-293T cells with KO of Arp2 or Arp3. (K,L) Western blot analysis confirms KO of Arp2 (K) or Arp3 (L), with GAPDH serving as the loading control. (M,N) Representative flow cytometry plots gated on mCherry$^+$ cells. (O,P) Quantifications of HR efficiency (GFP$^+$% of mCherry$^+$ cells); data represent the mean ± SD of three independent experiments. For (M,N), statistical significance relative to the wild-type (WT) control was determined by unpaired *t*-test (ns, not significant; *$p < 0.05$; ***$p < 0.001$; ****$p < 0.0001$).

5. Limitations

Several limitations should be kept in mind. First, all our experiments are *in vitro*—using gastric cancer cell lines and HEK-293T cells—so we cannot say how the combination would behave in a living animal. The lack of *in vivo* data means it remains unknown about systemic toxicity, pharmacokinetics, or the tumor microenvironment's influence. Animal studies (xenografts or PDX models) are clearly needed next. Second, because gastric cancer cells are notoriously hard to transfect, our HR assays had to be done in HEK-293T cells instead. While the results are consistent, we still need direct evidence of HR impairment in gastric cancer models with Arp2/3 perturbation. Also, we noticed that knocking out Arp2/3 changed cell shape and adhesion, pointing to its broader cytoskeletal roles [29]—this raises the question of whether inhibiting Arp2/3 therapeutically might cause unwanted side effects beyond blocking DNA repair.

6. Conclusions

We identified the Arp2/3 complex as a novel and viable therapeutic target for enhancing PARPi efficacy in gastric cancer cells. By demonstrating that CK666-induced inhibition of Arp2/3 compromises HR repair and establishes a synthetic lethal interaction with PARP blockade, we provide a robust preclinical rationale for a new combination therapy. This strategy not only promises to enhance antitumor efficacy, but also offers a potential path to reduce PARPi-related toxicities and overcome resistance. Future studies employing patient-derived xenografts and *in vivo* models will be essential to translate these promising *in vitro* findings into a viable therapeutic approach for gastric and other HR-proficient cancers.

Abbreviations

PARP, poly(ADP-ribose) polymerase; PARPi, PARP inhibitor; HR, homologous recombination; DSB, double-strand break; SSB, single-strand break; KO, knockout; IC_{50}, half-maximal inhibitory concentration; FBS, fetal bovine serum; CCK-8, Cell Counting Kit-8; CI, Combination Index; γH2AX, gamma H2A histone family member X.

Availability of Data and Materials

The data and materials that support the findings of this study are available from the corresponding authors upon reasonable request.

Author Contributions

Conceptualization: ZHD, JX; Data Curation: WLL, XYP, and ZHD; Methodology: WLL, XYP, TW, JX and ZHD; Formal Analysis: WLL, XYP, and XH; Investigation: WLL, XYP, YJL, YPL, XH, MS, QL, XYS, JQW, EMZ, and YHL; Validation: WLL and XYP; Visualization: WLL, XYP, TW, JX and ZHD; Resources: TW and ZHD; Writing – Original Draft: WLL, XYP, and TW; Writing – Review & Editing: TW, and ZHD; Supervision: ZHD; Project Administration: JX, TW, and ZHD; Funding Acquisition: JX, TW, and ZHD. All authors contributed to editorial changes in the manuscript. All authors read and approved the final manuscript. All authors have participated sufficiently in the work and agreed to be accountable for all aspects of the work.

Ethics Approval and Consent to Participate

Not applicable.

Acknowledgment

We are grateful to Professor Daniel D. Billadeau (Mayo Clinic College of Medicine, MN, USA) for kindly providing the pSpCas9(BB)-2A-Puro (PX459) V2.0 and pCI2-HA-mCherry plasmids.

Funding

This work was supported by the Heilongjiang Provincial Natural Science Foundation of China (LH2024H082), the Qiqihar Medical Institute Foundation (QMSI2024M-10 and 2025-ZDPY-002), the Education Department Foundation of Heilongjiang Province (2024-KYYWF-0339), and the Construction Project of Dominant Characteristic Disciplines of Qiqihar Medical University (QYZDXK-003).

Conflicts of Interest

The authors declare no conflicts of interest.

Declaration of AI and AI-Assisted Technologies in the Writing Process

During the preparation of this work, the authors used DeepSeek to improve readability and language. After using this tool, the authors reviewed and edited the content as needed and take full responsibility for the final content of the publication. The graphical abstract for this manuscript was created using the AI-based image generation tool GPT-image2. The tool was used to analyse the core content of our study, and we iteratively refined the output through multiple rounds of adjustment to ensure that the final illustration accurately and concisely represents our key findings. We have reviewed and take full responsibility for the final content.

Supplementary Material

Supplementary material associated with this article can be found, in the online version, at https://doi.org/10.31083/FBL51619.

References

[1] Bray F, Laversanne M, Sung H, Ferlay J, Siegel RL, Soerjomataram I, et al. Global cancer statistics 2022: GLOBOCAN

estimates of incidence and mortality worldwide for 36 cancers in 185 countries. CA: A Cancer Journal for Clinicians. 2024; 74: 229–263. https://doi.org/10.3322/caac.21834

[2] Yang Q, Xu D, Yang Y, Lu S, Wang D, Wang L. Global, Regional, and National Burden of Gastric Cancer in Adolescents and Young Adults, 1990-2019: A Systematic Analysis for the Global Burden of Disease Study 2019. The American Journal of Gastroenterology. 2024; 119: 454–467. https://doi.org/10.14309/ajg.0000000000002551

[3] Yu X, Zhang Y, Luo F, Zhou Q, Zhu L. The role of microRNAs in the gastric cancer tumor microenvironment. Molecular Cancer. 2024; 23: 170. https://doi.org/10.1186/s12943-024-02084-x

[4] Zu D, Bao Q, He H, Zhong Y, Deng M, Hu Y, et al. APOL2 Stabilizes Ku80 to Confer NHEJ-Mediated Radioresistance in Gastric Cancer. Advanced Science (Weinheim, Baden-Wurttemberg, Germany). 2025; 12: e06294. https://doi.org/10.1002/advs.202506294

[5] Langelier MF, Eisemann T, Riccio AA, Pascal JM. PARP family enzymes: regulation and catalysis of the poly(ADP-ribose) post-translational modification. Current Opinion in Structural Biology. 2018; 53: 187–198. https://doi.org/10.1016/j.sbi.2018.11.002

[6] Shao Z, Lee BJ, Zhang H, Lin X, Li C, Jiang W, et al. Inactive PARP1 causes embryonic lethality and genome instability in a dominant-negative manner. Proceedings of the National Academy of Sciences of the United States of America. 2023; 120: e2301972120. https://doi.org/10.1073/pnas.2301972120

[7] Shi L, Dasovich M, Horton JR, Liu H, Zhan Q, Manickavinayaham S, et al. Nuclear poly(A)-binding protein and nucleolin utilize their RNA recognition motifs to read PAR chains. Nucleic Acids Research. 2025; 53: gkaf1090. https://doi.org/10.1093/nar/gkaf1090

[8] Ray Chaudhuri A, Nussenzweig A. The multifaceted roles of PARP1 in DNA repair and chromatin remodelling. Nature Reviews. Molecular Cell Biology. 2017; 18: 610–621. https://doi.org/10.1038/nrm.2017.53

[9] Demin AA, Hirota K, Tsuda M, Adamowicz M, Hailstone R, Brazina J, et al. XRCC1 prevents toxic PARP1 trapping during DNA base excision repair. Molecular Cell. 2021; 81: 3018–3030.e5. https://doi.org/10.1016/j.molcel.2021.05.009

[10] Caldecott KW. Causes and consequences of DNA single-strand breaks. Trends in Biochemical Sciences. 2024; 49: 68–78. https://doi.org/10.1016/j.tibs.2023.11.001

[11] Li G, Lin SS, Yu ZL, Wu XH, Liu JW, Tu GH, et al. A PARP1 PROTAC as a novel strategy against PARP inhibitor resistance via promotion of ferroptosis in p53-positive breast cancer. Biochemical Pharmacology. 2022; 206: 115329. https://doi.org/10.1016/j.bcp.2022.115329

[12] Kimble MT, Sane A, Reid RJD, Johnson MJ, Rothstein R, Symington LS. Repair of replication-dependent double-strand breaks differs between the leading and lagging strands. Molecular Cell. 2025; 85: 61–77.e6. https://doi.org/10.1016/j.molcel.2024.10.032

[13] Lim J, Ju YS. Leveraging Whole-Exome Sequencing and Mutational Signatures to Detect Homologous Recombination Deficiency in Cancer. Cancer Research. 2025; 85: 2348–2350. https://doi.org/10.1158/0008-5472.CAN-25-2105

[14] Murciano-Goroff YR, Schram AM, Rosen EY, Won H, Gong Y, Noronha AM, et al. Reversion mutations in germline BRCA1/2-mutant tumors reveal a BRCA-mediated phenotype in non-canonical histologies. Nature Communications. 2022; 13: 7182. https://doi.org/10.1038/s41467-022-34109-8

[15] Hu X, Zhang J, Zhang Y, Jiao F, Wang J, Chen H, et al. Dual-target inhibitors of poly (ADP-ribose) polymerase-1 for cancer therapy: Advances, challenges, and opportunities. European Journal of Medicinal Chemistry. 2022; 230: 114094. https://doi.org/10.1016/j.ejmech.2021.114094

[16] Zagelbaum J, Schooley A, Zhao J, Schrank BR, Callen E, Zha S, et al. Multiscale reorganization of the genome following DNA damage facilitates chromosome translocations via nuclear actin polymerization. Nature Structural & Molecular Biology. 2023; 30: 99–106. https://doi.org/10.1038/s41594-022-00893-6

[17] Zhou FY, Ashton M, Jiang Y, Arora N, Clark K, Fitzpatrick KB, et al. Arp2/3 and type-I myosins control chromosome mobility and end-resection at double-strand breaks in S. cerevisiae. Nature Communications. 2025; 16: 7212. https://doi.org/10.1038/s41467-025-62377-7

[18] Schrank BR, Aparicio T, Li Y, Chang W, Chait BT, Gundersen GG, et al. Nuclear ARP2/3 drives DNA break clustering for homology-directed repair. Nature. 2018; 559: 61–66. https://doi.org/10.1038/s41586-018-0237-5

[19] Tang Z, Kang B, Li C, Chen T, Zhang Z. GEPIA2: an enhanced web server for large-scale expression profiling and interactive analysis. Nucleic Acids Research. 2019; 47: W556–W560. https://doi.org/10.1093/nar/gkz430

[20] Karlsson M, Zhang C, Méar L, Zhong W, Digre A, Katona B, et al. A single-cell type transcriptomics map of human tissues. Science Advances. 2021; 7: eabh2169. https://doi.org/10.1126/sciadv.abh2169

[21] Dimchev V, Lahmann I, Koestler SA, Kage F, Dimchev G, Steffen A, et al. Induced Arp2/3 Complex Depletion Increases FMNL2/3 Formin Expression and Filopodia Formation. Frontiers in Cell and Developmental Biology. 2021; 9: 634708. https://doi.org/10.3389/fcell.2021.634708

[22] Zhang L, Nie Y, Tang T, Lu Y, Li W, Hong X, et al. Nuclear VPS35 attenuates NHEJ repair by sequestering Ku protein. Molecular Medicine (Cambridge, Mass.). 2025; 31: 222. https://doi.org/10.1186/s10020-025-01288-1

[23] Zhang LP, Nie YH, Tang T, Zheng AX, Hong X, Wang T. Analysis of Nonhomologous End Joining and Homologous Recombination Efficiency in HEK-293T Cells using GFP Based Reporter Systems. Journal of Visualized Experiments : JoVE. 2024; 10.3791/66501. https://doi.org/10.3791/66501

[24] Wang Y, Zheng K, Huang Y, Xiong H, Su J, Chen R, et al. PARP inhibitors in gastric cancer: beacon of hope. Journal of Experimental & Clinical Cancer Research : CR. 2021; 40: 211. https://doi.org/10.1186/s13046-021-02005-6

[25] Hanna D, Chopra N, Hochhauser D, Khan K. The role of PARP inhibitors in gastrointestinal cancers. Critical Reviews in Oncology/hematology. 2022; 171: 103621. https://doi.org/10.1016/j.critrevonc.2022.103621

[26] Yu L, Wu D. SMARCA2 and SMARCA4 Participate in DNA Damage Repair. Frontiers in Bioscience (Landmark edition). 2024; 29: 262. https://doi.org/10.31083/j.fbl2907262

[27] Wainberg ZA, Singh AS, Konecny GE, McCann KE, Hecht JR, Goldman J, et al. Preclinical and Clinical Trial Results Using Talazoparib and Low-Dose Chemotherapy. Clinical Cancer Research : an Official Journal of the American Association for Cancer Research. 2023; 29: 40–49. https://doi.org/10.1158/1078-0432.CCR-22-1553

[28] Chu YY, Chen MK, Wei Y, Lee HH, Xia W, Wang YN, et al. Targeting the ALK-CDK9-Tyr19 kinase cascade sensitizes ovarian and breast tumors to PARP inhibition via destabilization of the P-TEFb complex. Nature Cancer. 2022; 3: 1211–1227. https://doi.org/10.1038/s43018-022-00438-2

[29] Derivery E, Gautreau A. Generation of branched actin networks: assembly and regulation of the N-WASP and WAVE molecular machines. BioEssays : News and Reviews in Molecular, Cellular and Developmental Biology. 2010; 32: 119–131. https://doi.org/10.1002/bies.200900123